The fate and contamination of trace metals in soils exposed to a railroad used by Diesel Multiple Units: Assessment of the railroad contribution with multi-tool source tracking

Jacek Szmagliński [a],[1], Nicole Nawrot [a],[*],[1], Ksenia Pazdro [b], Jolanta Walkusz-Miotk [b], Ewa Wojciechowska [a]

[a] Gdańsk University of Technology, Faculty of Civil and Environmental Engineering, Narutowicza 11/12, 80-233 Gdańsk, Poland
[b] Institute of Oceanology of the Polish Academy of Sciences, Marine Geotoxicology Laboratory, Powstańców Warszawy 55, 81-712 Sopot, Poland

HIGHLIGHTS

- Tracking connection between railroad operation and trace metals in soils
- Statistical analyses and Pb isotope ratios applied as tools
- Cr supplementation associated with the specificity of railroad geometrical layout
- Coal combustion as a source of Pb and correlated metals: Zn, Cu, Cd
- Lower environmental footprint exhibited by railway than road transport

GRAPHICAL ABSTRACT
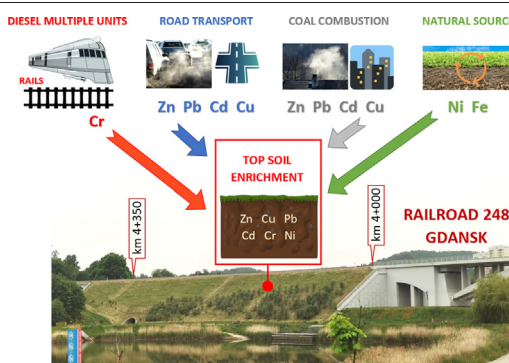
ABSTRACT

Soil samples from cut slopes from lightly loaded railway lines used by Diesel Multiple Units for 5 years in Gdansk (Poland) were collected and analyzed for trace metals (TMs): Zn, Pb, Cd, Ni, Cr, Cu, and Fe. The main aim was to assess soil enrichment, contamination status, and distribution of TMs relative to the distance from the railway track. Extensive source tracking analyses were performed using cluster analysis (CA) and the Pb isotope ratios approach (^{206}Pb, ^{207}Pb, and ^{208}Pb). Soil samples were affected by Cr, Cu, Pb, and Zn (max values in mg/kg d.w.: 31.1, 145, 80.5, and 115, respectively). The Enrichment Factor showed moderate (Cr, Zn, Pb) to very severe (Cu) enrichment. CA allowed TMs to be divided into two general groups: a) containing Zn, Pb, Cd with slight interaction with Cu; and b) containing Fe and Ni with slight interaction with Cr. Correlation analyses indicated Cr as an outlying TM delivered from a separate source associated with the specificity of the construction of railroad 248, where alloys containing Cr were used to counteract increasing wear-and-tear of the rails. Pb isotopic ratios in the ranges of 1.16–1.20 (^{206}Pb/^{207}Pb) and 2.05–2.10 (^{208}Pb/^{206}Pb) corresponded to anthropogenic supplementation (coal combustion, road vehicles, and railroad transport) of Pb and Pb-correlated TMs (Zn, Cd, and partly Cu). Despite the research focus on the impact of the railroad contribution, a comparison with other forms of transport indicated that road transport appeared to have a higher contributing factor to TM pollution at the investigated site. This general conclusion again emphasizes the lower environmental footprint exhibited by railway transport in comparison to road transport.

© 2018 Elsevier B.V. All rights reserved.

* Corresponding author.
  E-mail address: nicnawro@pg.edu.pl (N. Nawrot).
[1] Jacek Szmagliński and Nicole Nawrot contributed equally to this work.

1. Introduction

Globalization and economic growth in recent decades have led to dynamic development of transport. Transportation not only has a direct negative contribution to human health and life due to the risk of accidents (Jamroz et al., 2019; Kustra et al., 2019; Budzynski et al., 2019) but it also has a high environmental footprint, and it is beyond any doubt one of the major pathways for pollutants to enter air, water and soil (Yan et al., 2018). Pollution is associated with the combustion of liquid fuels, dust emission related to the wear of mechanical elements of vehicles and roads, followed by secondary dust emission related to particles displaced by air movement caused by a passing vehicle (Adamiec et al., 2016; Crosby et al., 2014; German and Svensson, 2018; Liu et al., 2018b; Nawrot et al., 2020a). Transport is, therefore, a source of both point emission (production plants and refineries) and linear emission (roads, railways, etc.). The latter affects areas in the vicinity of traffic corridors and, typically for no-point emissions, is usually difficult to assess and properly manage. Exhaust gases and the effects of vehicle and road wear are a source of harmful substances such as oxides of carbon, nitrogen, and sulphur (from 10 to 40% of total emissions), suspended dust, trace metals (TMs) (Mohsen et al., 2018; Wojciechowska et al., 2019a,b), polycyclic aromatic hydrocarbons (PAHs) (Liu et al., 2020), polychlorinated biphenyls (PCBs) (Stojic et al., 2017), etc. Emission magnitude depends strongly on the means of transport. Currently, in Europe, about 75% of goods are transported by road, while approximately 19% are transported by rail, and the remainder is transported by water (EC EUROPA). In the case of passenger transport, private road transport constitutes 62–96% and rail transport 0–17%, depending on the country (EEA EUROPA). Due to the clear disproportion in passenger-kilometers and ton-kilometers, as well as the emissivity of each means of transport, for many years research has focused on the impact of road transport (Chen et al., 2010; Hong et al., 2018; Zafra et al., 2017). Some other studies examined air transport, where toxic compounds are mostly released in the vicinity of runways (Brtnický et al., 2020). Research concerning the pathways for contaminants originating from rail transport have most often focused on dust emissions from the contact of wheels with rails, the wear of the overhead lines and slide plates of pantographs (Weerakkody et al., 2017), as well as the content of dust in the atmosphere of closed systems, such as metro or underground rail systems (Nieuwenhuijsen et al., 2007). Contaminants emitted from rail transport can cause health problems, which have been investigated by, among others, Loxham and Nieuwenhuijsen (2019). Some earlier studies concerning TMs in urban areas selected Cr as a characteristic component in the bottom sediments of retention tanks located in the vicinity of railroads (Nawrot et al., 2020b).

The particularly important toxic elements deposited in the soils of railway cut slopes are TMs. Zn, Pb, Cr, Cd, Ni, and Cu which are of research interest in areas near railroads (Brtnický et al., 2020). TM occurrence in the environment stamps a specific footprint due to their non-biodegradable nature. TM enrichment should be evaluated in the context of their natural persistence in the soil, for instance by using calculation indices like the Pollution Load Index (PLI), Contamination Factor (CF), Enrichment Factor (EF), or Geochemical Index (Igeo) (Kowalska et al., 2018; Weissmannová and Pavlovský, 2017; Wojciechowska et al., 2019a,b). Scanning for TM enrichment in soils is an effective tool that accurately reflects the existing contamination of the surrounding environment and should be of interest to decision makers. Statistical methods to obtain data for different matrices are frequently used to verify the possible sources of contamination (González-Macías et al., 2014; Wang et al., 2015). An advanced method for source tracking of TMs in soil relies on the use of stable isotopes, which provide a "signature" of elements (Gao et al., 2018). In environmental science, the isotope ratios $^{206}Pb/^{204}Pb$, $^{206}Pb/^{207}Pb$, $^{208}Pb/^{206}Pb$ and $^{208}Pb/^{207}Pb$ offer the most useful and reliable information due to their abundance and precise analytical determination. The Pb isotope signature in surface soil samples yields some basic information on Pb's origin, e.g. whether it is from coal-fired power plants, burning of fossil fuels, waste incineration, mining, etc. (Cheema et al., 2020). The use of Pb isotope analysis can also indirectly point out the sources of other TMs since the abundance of various metals can be linked (Nawrot et al., 2020a). The application of Pb isotopes to track Pb and associated TM origin is a relatively novel approach and, to the authors' knowledge, has not been applied before to examine the impact of railroad transport on soil.

Combining methods of contamination assessment and source tracking of TMs benefits an authoritative assessment of soils. This approach supports decision-making and good management practices that might prevent environmental deterioration.

The overarching aim of this study is to assess the impact of railroad on the fate of TMs and contamination in soils at a lightly loaded railway line with cut slopes, which was built between 2013 and 2015. The railway is used by diesel trains. The specific research objectives were as follows: 1) to assess TM (Pb, Zn, Cd, Cr, Ni, Cu, and Fe) enrichment and distribution in the surface soil layer of railway embankments relative to the distance from the railway track; 2) to evaluate the contamination status of surrounding soils including the differences between the natural and anthropogenic levels of TMs of an analyzed area; and 3) to track the TM sources by employing statistical and Pb isotopic ratio analyses ($^{206}Pb/^{207}Pb$, $^{208}Pb/^{206}Pb$, and $^{207}Pb/^{208}Pb$). The findings of this study contribute to an indication of anthropogenic TM sources and the assessment of the overall impact of transportation modes on the environment.

2. Materials and methods

2.1. Study area and specific feature of the testing section

The railroad section tested in this study is located along railway line no. 248 in Gdansk, northern Poland. Railway line 248 was built between 2013 and 2015. Due to the challenging terrain, railway line 248 has the parameters of a mountain line (very large longitudinal gradients and small radius of curves). Currently, 46 pairs of trains run daily on railway line 248 in the research area. The trains consist of Diesel Multiple Units (DMUs) weighing from 82 to 108 t (108 Mg). Hence, the average daily truckload is 4600 t (4600 Mg), which gives an annual load of around 1.5 Tg. This classifies the railway line as very lightly loaded. The maximum speed of the trains is 120 km/h. Railway line 248, following regulations enforced in Poland (Regulation of the Minister, 1998), is classified as Class 1 (on a four-level scale, where 0 is the highest class and 3 is the lowest). Since opening, the number of transported passengers has been gradually increasing and amounted to 400,000 people per month at the end of 2019. Electrification of the railway line will start in 2021, and the completion of work is planned for 2023. After electrification, the trains are expected to be faster and run more frequently, which should attract even more travelers.

2.2. Soil sampling strategy

Three testing sections (Fig. 1) were selected to extract soil samples in the close vicinity of the railway track. The boundary of the track is a ballast structure and the track itself was made as a continuous welded track, which consists of rails with 49E1 profiles, according to European standard EN 13674-1 on prestressed concrete sleepers of the PS-93/W-14/1435/49E1 type with a W-14 fastening system.

The parameters of the testing sites presented in Fig. 1 are as follows:

- Test site 1 at 4 + 000 km (Fig. S. 1a): a double-track section located on a horizontal curve with a radius of about 800 m and a longitudinal slope of 18‰. Due to the very small radius of the curve hardened rails made from heat-treated steel were used here. The cross-section is located near a road with very heavy traffic (the traffic flow is more than 5000 vehicles per hour in the peak) (Via Vistula, 2016). Three soil sampling points were located at this site: at the base of the embankment (native soil) – sample no. 11; at the half-height of
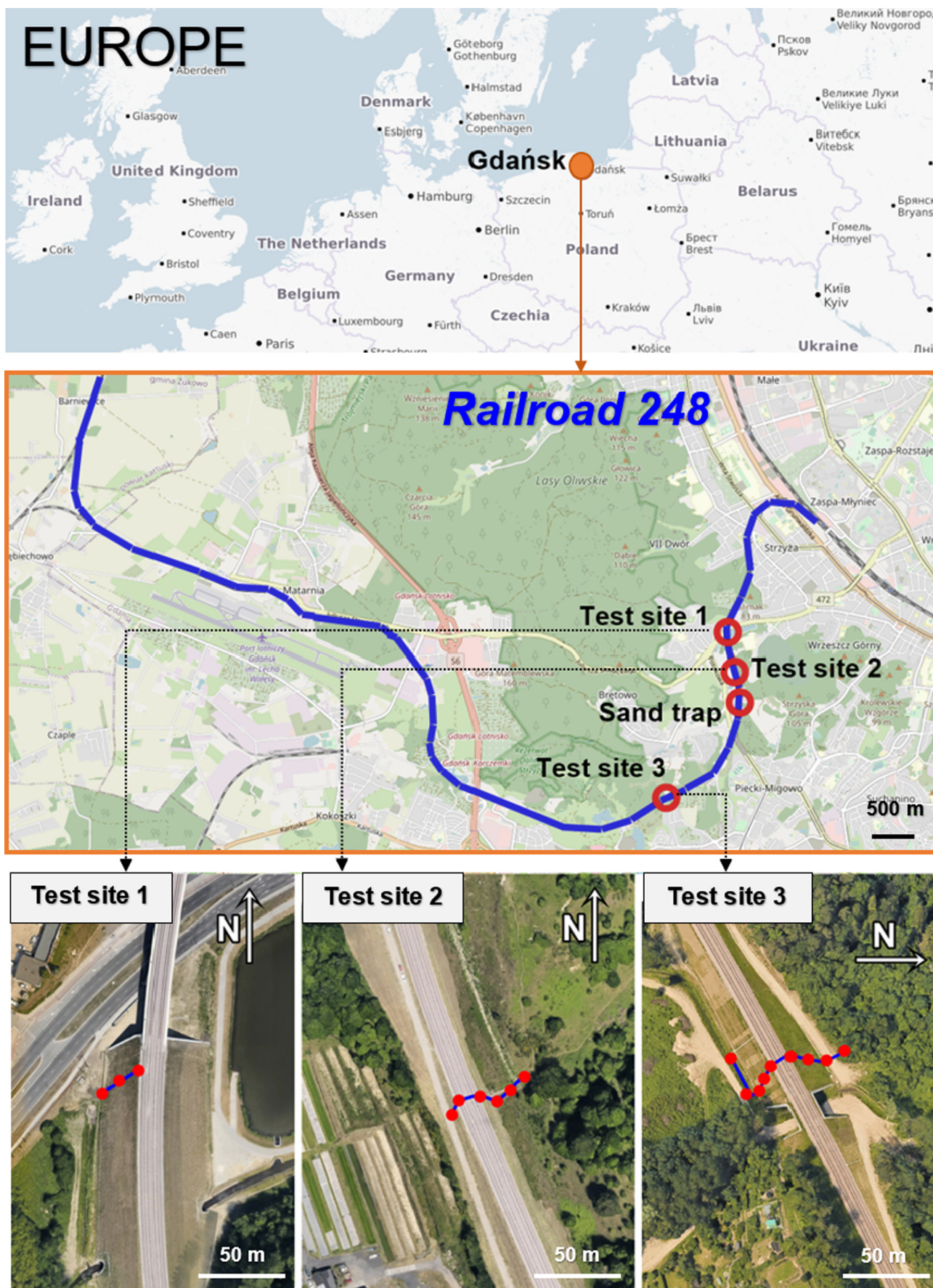
Fig. 1. Location of the testing sites. Figure elaborated using Google maps and OpenStreetMap.

the embankment (embankment soil) – sample no. 12; and at the crest (sand and gravel mix 0–31.5 mm aggregate) – sample no. 13. This test site was chosen to verify the possible influence of the neighbouring intersection on metal soil supplementation on railway embankments.

- Test site 2 at 4 + 350 km (Fig. S. 1b): a double-track section located on a horizontal curve with a radius of about 800 m and a longitudinal slope of 18‰. Here, again, hardened rails were used due to the very small radius of the curve. The cross-section is located in an undeveloped area. Seven soil sampling points were selected, of which a total of six were: at the base of the embankment (native soil) – sample no. 21; at the crest (sand and gravel mix 0-31.5 mm aggregate) – samples no. 22 and 23; at the bottom of the drainage ditch (dry, native soil) – sample no. 24; and at the excavation slope (native soil) – samples no. 25 and 26. One soil sample was extracted from the sand trap located at 4 + 640 km – sample no. 27 (not shown in Fig. S 1b).

- Test site 3 at 6 + 600 km (Fig. S 1c): a double-track section located on a horizontal curve with a radius of about 3000 m and a longitudinal slope of 13‰. Due to the radius of the curve typical rails were used there. The cross-section is located in an undeveloped area. Nine soil sampling points were selected: at the base of the embankment (native soil) – samples no. 31 and 36; at the half-height of the embankment (embankment soil) – samples no. 32 and 35; at the crest (sand and gravel mix 0–31,5 mm aggregate) – samples no. 33 and 34; at a 10 m distance from the base of the embankment (native soil) – sample no. 37; and from the drainage ditch – samples no. 38 and 39.

The soil samples were collected by using a plastic sampler. At each sampling point, the top layer of soil (approx. 5 cm in depth) from 3 to 4 crosswise located sites (within the 0.25 m^2 area of the sampling point) were extracted and mixed. Each mixed soil sample was packed into a PE bag and immediately delivered to the laboratory. The sampling process took place in June 2020.

2.3. Chemical analyses

2.3.1. Determination of trace metals

After collection, the soil samples were homogenized, transferred to Petri dishes, and lyophilized. To determine the concentration of seven TMs (Zn, Cu, Pb, Cd, Ni, Cr, and Fe) a soil subsample of 0.5 g (0.001 g accuracy) was digested with $HClO_4$, HF, and HCl (3:2:1; Suprapur) in Teflon bombs in an oven (140 °C), for 4 h, according to the procedure described by Vallius and Leivuori (1999). The solution was then evaporated to dryness and 5 mL of concentrated Suprapur HNO_3 was added and evaporated. The dried residue was dissolved in 5 mL of Suprapur 0.1 M HNO_3 and placed in polyethylene tubes. Dilutions of ×10, ×100, and ×1000 were prepared and analyzed in an inductively coupled plasma mass spectrometer (ICP-MS; Perkin–Elmer ELAN 9000). The results are presented as mg/kg d.w. (d.w. – dry weight). The measurements were replicated three times. Quality control was assured by analyzing a certified reference material and "blanks", according to the same procedure. Recoveries were in the range of 92–103%, depending on the individual metals. The precision, given as Relative Standard Deviation, was in the range of 3–5%. The detection limits (LOD) of each element were calculated as Blank + 3·SD, where SD values were the standard deviations of the blank samples ($n = 5$). LODs were as follows: Pb - 1.0 mg/kg, Zn -0.5 mg/kg, Cr - 1.5 mg/kg, Ni - 0.7 mg/kg, Cu - 0.3 mg/kg, and Cd - 0.1 mg/kg.

2.3.2. Pb isotopic ratios

Stable lead isotopes (^{206}Pb, ^{207}Pb and ^{208}Pb) were measured using a Perkin–Elmer Sciex ELAN 9000 ICP-MS and the ^{206}Pb/^{207}Pb, ^{208}Pb/^{206}Pb, ^{208}Pb/^{207}Pb ratios were calculated. Together with all sample sets the repeated digestion and analyses of the certified standard material NBS-981 ($n = 5$) was performed to validate measurement accuracy. The results were satisfactory and recovery was >98%. The mean ^{206}Pb/^{207}Pb ratio for NBS-981 was 1.09413 ± 0.00407 (certified value = 1.09333)

and the mean ^{208}Pb/^{206}Pb ratio was 2.14269 ± 0.00859 (certified value = 2.16810). Three blank samples (containing only chemicals) were measured with every ten samples.

LODs were as follows: ^{206}Pb - 0.007 µg/dm^3, ^{207}Pb - 0.007 µg/dm^3, and ^{208}Pb - 0.007 µg/dm^3. Mean RSD was calculated from a triple analysis (separate digestion and measurement of 3 parallel subsamples) of every third sample. It was equal to 0.17% for the ^{206}Pb/^{207}Pb ratio and 0.53% for the ^{208}Pb/^{206}Pb ratio.

2.4. Soil contamination status

A geochemical assessment of the soil environmental status was performed using several soil indices. A Contamination Factor (CF) was applied as an index which provides information about a single metal's contribution to the contamination status (Hakanson, 1980; Tomlinson et al., 1980) according to formula (1).

$$CF = \frac{C_{Sample}}{C_{Background}} \tag{1}$$

where C_{Sample} is the metal content in the analyzed soil sample and $C_{Background}$ is the metal content in soil referred to as preindustrial (this value informed the environmental background status). The $C_{Background}$ values were established based on the provided by the Central Geological Database in Poland (GeoLOG application) for the surface layer of soil (mean in mg/kg d.w. for the examined area: Zn – 45, Cu – 4.2, Cd – 0.5, Pb – 16.5, Ni – 5.6, Cr – 5.6).

For a comprehensive evaluation of soil quality in accordance with all the analyzed TMs, the Pollution Load Index (PLI) was calculated according to formula (2) (Tomlinson et al., 1980; Weissmannová and Pavlovský, 2017).

$$PLI = \sqrt[n]{CF_1 \cdot CF_2 \cdot \ldots \cdot CF_n} \tag{2}$$

where CF_n is the CF described above and n is the number of metals studied.

Moreover, to further analyze the obtained results, an Enrichment Factor (EF) was calculated. This index considers the normalization of TM concentration and enables the identification of those areas of the examined soils in which increased amounts of anthropogenic chemical components have accumulated, regardless of their granulometry (Sakan et al., 2014). Formula (3) presents the computational approach for EF (Zhang et al., 2012).

$$EF = \frac{\frac{C_{Sample}}{C_{Background}}}{\frac{C_{refSample}}{C_{refBackground}}} \tag{3}$$

where C_{Sample} and $C_{Background}$ are the same values as described above, while $C_{refSample}$ and $C_{refBackground}$ represent the normalizer element concentration in the analyzed sample and environmental background, respectively. The normalizer element was Fe due to its common abundance in the earth's crust. The $C_{refBackground}$ value, established as a mean concentration of Fe (15,866 mg/kg d.w.), was used in calculations for all the analyzed samples (to take into account the possible influence of extraneous soil used in the formation of railway embankments).

The classes of soil quality described with the use of CF, PLI, and EF are presented in Table S.1.

2.5. Source tracking using Pb isotopic ratio

A two-isotope plot (^{206}Pb/^{207}Pb vs. ^{208}Pb/^{206}Pb) was applied to distinguish separate Pb sources. This approach allows for a more precise identification of separate Pb sources. The values of the ^{206}Pb/^{207}Pb and ^{208}Pb/^{206}Pb ratios reported in the literature are presented in Table 1.

Table 1
The Pb isotopic ratios (^{206}Pb/^{207}Pb and ^{208}Pb/^{206}Pb) for different sources of Pb in the environment.

Pb isotope ratio	Value	Description of the source of Pb origin	References
^{206}Pb/^{207}Pb	0.96–1.2	Anthropogenic	(Sun et al., 2018)
	>1.2	Natural	
	1.22	Old and uncontaminated polish rocks	(Zaborska, 2014)
	1.16–1.17	Leaded gasoline used in central and eastern Europe	(Yao et al., 2015)
	1.14–1.15	Unleaded gasoline	
	1.14–1.16	Diesel	
	1.10	Unleaded gasoline and diesel from Russia	(Chrastný et al., 2018)
	1.15–1.17	Mechanical wastes derived from vulcanisation, tyre balancers, tyre scraps, and wheel alignment systems	(Nawrot et al., 2020a)
	1.17–1.19	European coal	(Komárek et al., 2008)
^{208}Pb/^{206}Pb	<2.08	Natural/coal source	(Zaborska and Zawierucha, 2016)
	>2.08	Contribution of gasoline Pb	
	2.05–2.08	Mechanical wastes derived from vulcanisation, tyre balancers, tyre scraps, and wheel alignment systems	(Nawrot et al., 2020a)

2.6. Statistical analyses

Non-parametric Spearman correlation analysis was used for variables (TMs) to assess their interdependence. Correlations with $p < 0.05$ were considered to be significant. Ward's cluster analysis (CA) for the measured TMs was carried out to identify the relationship between seven elements and their probable sources. The data analysis was performed using STATISTICA 13 (StatSoft) software.

3. Results & discussion

3.1. Trace metal content in the soil

TM content (mean ± SD) in the analyzed samples is presented in Table 2. The general scenario was that TM concentration decreased in the following order: Fe > Zn > Pb > Cr > Cu > Ni > Cd. In comparison to the background TM concentrations in the area under consideration, the highest excess in the analyzed soil samples was noted for Cr, Cu, and Zn: 5.6, 5.5, and 2.2 times for Test site 1, 5.2, 6.3, and 1.3 times for Test site 2, and 4.2, 34.5, and 2.6 times for Test site 3, respectively. Stojic et al. (2017), in research performed in Serbia, found increased concentrations of Zn and Cu near to a railroad (within 1 km) and

concluded that railways, in general, contribute these TMs to surrounding soils. The Cu and Zn concentrations reported by Stojic et al. (2017) ranged between 8.73–216 mg/kg d.w. and 12.69–191 mg/kg d.w., respectively. In our study, the maximum observed contents of these TMs were 145 mg/kg d.w. for Cu and 115 mg/kg d.w. for Zn. The railroad investigated in our study is relatively new, compared to the 130-year-old railway in Serbia and also relatively lightly loaded, which could account for the differences in TM concentrations. An important observation from our research was that Pb concentrations were higher in comparison to other studies – the maximum values measured in this investigation were 65 mg/kg d.w. at Test site 1, 41.1 mg/kg d.w. at Test site 2, and 80.5 mg/kg d.w. at Test site 3, while Stojic et al. (2017) reported a maximum Pb value of 36.4 mg/kg d.w. and Zhang et al. (2012) reported a maximum Pb value of 41.8 mg/kg d.w. This higher Pb content may be associated with the specificity of the analyzed area, since the railway is located in a city district (only Test site 3 is further the city centre and is located in a forested area). In contrast, the above-mentioned studies analyzed soil samples collected close to railways crossing farmlands or natural landscape zones. However, the Ni and Cd concentrations in this study were at a relatively low level (3.28–13.2 mg/kg d.w. and 0.030–0.282 mg/kg d.w. for Ni and Cd, respectively), while Stojic et al. (2017) reported a Ni content ranging between 11.0 and 115 mg/kg d.w. and Cd content between 0.080 and 0.740 mg/kg

Table 2
Concentration of mean ± SD ($n = 3$) trace metals (TMs) (Cr, Ni, Cu, Cd, Pb, Zn, and Fe) in analyzed soil samples collected from the Testing sites 1–3 along railway line 248.

Sample	Trace metal mean ± SD concentration [mg/kg d.w.]						
	Cr	Ni	Cu	Cd	Pb	Zn	Fe
Test site 1							
11	20.5 ± 0.8	7.24 ± 0.29	22.9 ± 0.92	0.112 ± 0.004	65.0 ± 2.6	59.9 ± 2.4	12,945 ± 259
12	31.1 ± 1.2	6.03 ± 0.24	7.58 ± 0.30	0.100 ± 0.004	23.5 ± 0.9	35.2 ± 1.4	13,748 ± 275
13	26.8 ± 1.1	8.36 ± 0.33	20.2 ± 0.81	0.282 ± 0.011	60.6 ± 2.4	97.5 ± 3.9	20,082 ± 402
Test site 2							
21	29.3 ± 1.2	8.32 ± 0.33	26.5 ± 1.1	0.122 ± 0.005	41.1 ± 1.6	58.4 ± 2.3	19,267 ± 385
22	22.5 ± 0.9	9.53 ± 0.38	6.62 ± 0.26	0.090 ± 0.004	32.6 ± 1.3	37.5 ± 1.5	21,473 ± 429
23	23.9 ± 1.0	7.34 ± 0.29	8.64 ± 0.35	0.092 ± 0.004	22.9 ± 0.9	36.8 ± 1.5	14,303 ± 286
24	22.1 ± 0.9	3.28 ± 0.13	4.58 ± 0.18	0.056 ± 0.002	13.8 ± 0.6	20.3 ± 0.8	14,189 ± 284
25	22.3 ± 0.9	3.71 ± 0.15	4.96 ± 0.20	0.074 ± 0.003	15.6 ± 0.6	22.1 ± 0.9	11,667 ± 233
26	17.8 ± 0.7	3.99 ± 0.16	4.57 ± 0.18	0.074 ± 0.003	17.6 ± 0.7	20.3 ± 0.8	10,270 ± 205
27	9.61 ± 0.38	7.04 ± 0.28	12.6 ± 0.51	0.120 ± 0.005	22.7 ± 0.9	56.8 ± 2.3	11,705 ± 234
Test site 3							
31	21.6 ± 0.9	5.21 ± 0.21	145 ± 6	0.174 ± 0.007	64.1 ± 2.6	60.6 ± 2.4	15,170 ± 303
32	21.6 ± 0.9	8.24 ± 0.33	26.0 ± 1.0	0.274 ± 0.011	66.3 ± 2.7	88.8 ± 3.6	11,972 ± 239
33	19.0 ± 0.8	6.45 ± 0.26	11.5 ± 0.5	0.086 ± 0.003	38.0 ± 1.5	33.9 ± 1.4	11,919 ± 238
34	22.2 ± 0.9	8.67 ± 0.35	12.0 ± 0.5	0.092 ± 0.004	25.7 ± 1.0	52.7 ± 2.1	31,494 ± 630
35	23.5 ± 0.9	13.2 ± 0.53	34.3 ± 1.4	0.136 ± 0.005	80.5 ± 3.2	75.8 ± 3.0	19,476 ± 390
36	15.9 ± 0.6	5.17 ± 0.21	13.5 ± 0.5	0.120 ± 0.005	48.1 ± 1.9	115 ± 4.6	11,010 ± 220
37	23.7 ± 0.9	8.50 ± 0.34	21.4 ± 0.9	0.206 ± 0.008	57.6 ± 2.3	71.5 ± 2.9	14,881 ± 298
38	11.7 ± 0.5	7.86 ± 0.31	10.6 ± 0.4	0.068 ± 0.003	16.4 ± 0.7	34.7 ± 1.4	9428 ± 189
39	17.5 ± 0.7	7.62 ± 0.30	10.8 ± 0.4	0.030 ± 0.001	20.8 ± 0.8	21.5 ± 0.9	6989 ± 140
Background (in surface soils) (GeoLOG application)	5.60	5.60	4.20	0.500	16.5	45.0	
Local background							15,866

Table 3
Trace metal (TM) concentrations [mg/kg d.w.] in soil samples influenced by rail, road, and air transport across the world.

Site	Description	Concentration of TMs [mg/kg d.w.]						References
		Zn	Cu	Pb	Cd	Ni	Cr	
Railway transport								
Masovian Voivodeship, Poland	Railway line crossing a wooded area; built in 1936 as an electrified line; an important role in the national railway system; railway serves electric trains and freight (diesel) trains.	77 [a] 3.1 [d]	32 [a] 3.2 [d]	45 [a] 3.6 [d]	0.97 [a] 1.9 [d]	37.8 [a] 7.6 [d]	11.9 [a] 2.9 [d]	Radziemska et al., 2020
Serbia	Soil sampling at 0–0.5 km distance from a railroad built 130 years ago; section used for passenger and cargo traffic	12.69–191.4 [b] 61.27 [a] 0.48 [d]	8.73–215.7 [b] 41.46 [a] 1.02 [d]	12.91–36.44 [b] 24.16 [a] 0.30 [d]	0.08–0.74 [b] 0.38 [a] 0.52 [d]	14.16–115.5 [b] 48.99 [a] 1.35 [d]	10.32–64.26 [b] 36.46 [a] 0.36 [d]	Stojic et al., 2017
Qinghai–Tibet	D: soil sampling at 2–150 m distance from a railroad; relatively flat terrain; T: soil sampling at 2–200 m distance from the railroad; uniform vegetation and soil type associated with the regional landscape H: soil sampling at 2–200 m distance from the railroad; dominant landscapes in the Tibetan plateau;	D: 41.1 ± 11.9 [c] 0.55 [d] T: 81.8 ± 7.6 [c] 1.10 [d] H: 78.8 ± 8.7 [c] 1.06 [d]	D: 14.8 ± 1.5 [c] 0.65 [d] T: 31.1 ± 1.8 [c] 1.38 [d] H: 24.1 ± 1.9 [c] 1.07 [d]	D: 21.4 ± 6.5 [c] 0.82 [d] T: 26.1 ± 2.7 [c] 1.00 [d] H: 25.6 ± 3.1 [c] 0.98 [d]	D: 0.13 ± 0.09 [c] 1.37 [d] T: 0.19 ± 0.05 [c] 1.91 [d] H: 0.20 ± 0.09 [c] 2.07 [d]	D: 16.2 ± 2.9 [c] 0.69 [d] T: 33.6 ± 2.6 [c] 1.44 [d] H: 32.8 ± 2.8 [c] 1.40 [d]	D: 31.5 ± 5.3 [c] 0.52 [d] T: 71.2 ± 4.1 [c] 1.17 [d] H: 70.6 ± 6.2 [c] 1.16 [d]	Zhang et al., 2012
Abisco, Northern Sweden	Soil sampling at 0–1280 m distance from a railroad; railway transporting iron ore through an otherwise undisturbed, unpolluted birch forest	43–68 [b]	25–64 [b]	60–230 [b]				Goth et al., 2019
Sichuan Province, China	Soil samples collected on a cut slope affected by railway transportation for 5 years	137.2–168.9 [b] 158.0 ± 9.4 [c] 2.30 [d]	15.6–19.1 [b] 17.6 ± 0.9 [c] 0.66 [d]	25.8–87.1 [b] 49.2 ± 16.5 [c] 2.54 [d]	0.67–4.27 [b] 2.08 ± 0.94 [c] 20.8 [d]		20.3–64.3 [b] 35.6 ± 13.8 [c] 0.72 [d]	Chen et al., 2014
Road transport								
Europe	Roadside soils; at the distance of 0–5 m to the road edge	110–380 [b]	20–60 [b]	30–200 [b]	0.04–2.0 [b]	17–48 [b]	17–60 [b]	Werkenthin et al., 2014
Stockholm, Sweden	Area near a street in central Stockholm	41 [a] 7.8–118 [b]	57.6 [a] 12.8–171 [b]	7.2 [a] 1.5–15.4 [b]	0.12 [a] 0.015–0.32 [b]	2.9 [a] 0.26–7.5 [b]	6.1 [a] 1.13–18.3 [b]	Johansson et al., 2008
Edinburg, United Kingdom	Area near a two-lane road, with light traffic. A: near curb, B: 1 m from the curb.	A: 213 [a] 107–457 [b] 1.99 [d] B: 211 [a] 99–460 [b] 1.97 [d]	A: 57 [a] 22–122 [b] 1.30 [d] B: 79 [a] 26–220 [b] 1.80 d	A: 118 [a] 25–621 [b] 4.21 [d] B: 35 [a] 6–102 [b] 1.25 [d]	A: 1 [a] 0–2 [b] 1.00 [d] B: 2 [a] 1–4 [b] 2.00 [d]	A: 15 [a] 6–33 [b] 0.75 [d] B: 9 [a] 3–15 [b] 0.45 [d]	A: 16 [a] 5–76 [b] 2.00 [d] B: 15 [a] 6–29 [b] 1.88 [d]	Pal et al., 2010
Warsaw, Poland	Areas near to a highway			70–100 [b] 3.7 [d]	0.7–0.9 [b] 2.2 [d]	3.7–3.7 [b] 0.13 [d]	29–32 [b] 0.5 [d]	Lisiak-Zielinska et al., 2021
Turin, Italy	Soil samples at braking sites (BS) and acceleration sites (AC)	BS: 90–560 [b] AC: 170–300 [b]	BS: 60–380 [b] AC:100–490 [b]	BS:40–100 [b] AC: 30–170 [b]		BS: 180–270 [b] AC:180–500 [b]	BS: 350–420 [b] AC: 380–850 [b]	Padoan et al., 2017
Air transport								
Runway (airport) Warsaw, Poland	Landing site	3.96–1581 [b] 152 ± 239 [c] 6.1 [d]	2.58–41.3 [b] 14.0 ± 9.19 [c] 2.2 [d]	22.3–473 [b] 64.2 ± 66.9 [c] 3.2 [d]		3.67–32.6 [b] 8.83 ± 4.77 [c] 1.8 [d]		Brtnický et al., 2020
Runway (airport) Delhi, India	Landing site	142 ± 56.9 [c] 2.8 [d]	28.1 ± 6.11 [c] 2.2 [d]	42.9 ± 13.9 [c] 2.2 [d]	2.07 ± 1.21 [c] 25.9 [d]	42.9 ± 5.43 [c] 1.5 [d]	120 ± 46.1 [c] 1.9 [d]	Ray et al., 2012

Explanation to [a, b, c]: TM concentrations were presented as average value [a], min–max values [b], or mean ± SD [c] depending on the results presented by individual authors; Explanation to [d]: Contamination Factor, calculated based on the background concentration of TM presented by individual authors.

d.w. In the case of Cr the values observed in this study (9.61–31.1 mg/kg d.w.) in general were in a similar range to those obtained by Stojic et al. (2017) and Zhang et al. (2012): 10.3–64.2 mg/kg d.w. and 18.5–46.5 mg/kg d.w., respectively. According to the regulations set by the Polish Minister of the Environment (2016) for soil surface assessment, the concentrations observed in this study do not exceed the recommended limit values for terrain belonging to group IV (road and railroad lands) (these limit values are, in mg/kg d.w.: Cu – 600, Zn – 2000, Pb – 600, Cd – 15, Cr – 1000, Ni – 500).

3.2. Comparison of TM concentrations in soils with different types of transport

TM concentrations in soil samples obtained in this study were compared to other studies analyzing different means of transport: railway, road, and air transport (Table 3). Goth et al. (2019) reported increased Pb content (max 230 mg/kg d.w.) near a railway transporting iron ore through an otherwise undisturbed, unpolluted birch forest. Despite the similar period of use of the railroad studied in China (5 years) (Chen et al., 2014), results similar to this study were recorded only for Pb (up to 87 mg/kg d.w.). Zn, Cd, and Cr contents were higher than those observed in this study. TM supplementation to the soil in the vicinity of the railroad certainly does occur, although the final effect on soil pollution may depend on many factors, i.e. the type of fuel used, the land use around the railroad, its age as well as the initial TM content in soil at the analyzed site. TM contribution from other sources may also add to the overall concentration. In addition, the level of soil contamination should be referred to the geochemical background or preindustrial content of each studied TM. Taking into account the CF, the highest excess over the background value was recorded for Ni in Poland (CF = 7.6) (Radziemska et al., 2020) and Cd in China (CF = 20.8) (Chen et al., 2014).

Comparing the TM content in our study to the results obtained for soils affected by road transport in European countries (Pal et al., 2010; Werkenthin et al., 2014; Lisiak-Zielinska et al., 2021), it can be unequivocally stated that, in the latter case, the TM concentrations were much

higher. It was also demonstrated by Padoan et al. (2017) that the increase in TM content in soil samples is related to emissions caused by rapid changes in movement (acceleration and braking).

In the case of air transport high TM content was observed for Zn and Pb in Poland (Brtnický et al., 2020) and Cr and Cd in India (Ray et al., 2012) at landing sites. In the assessment of air transport pollution, the highest exceedance of background concentrations was recorded for Zn in Poland (CF = 6.1) (Brtnický et al., 2020) and Cd in India (CF = 25.9) (Ray et al., 2012).

3.3. Consideration of the contamination status consideration of soil in the area of the railway

To gain a more detailed understanding of TM contamination, CF, PLI, and EF values were calculated for the obtained data and presented in Table 4.

The general observation coming from CF calculations indicates that at all test sites there is considerable Cr contamination on crests and embankments. Moreover, at Test site 1, considerable Cu and Pb contamination was noted at the base of the embankment and the crest. At Test site 2 increased contamination status was observed for Cu in sample no. 21 located at the base of the embankment. In the case of Test site 3, on embankment locations (at the base and half-height of the embankment), increased Cu and Pb contamination was observed (especially in the case of Cu with very severe enrichment observed for samples no. 31, 32, and 35).

The PLI value gives a comprehensive assessment of the contamination status, which suggests the influence of anthropogenic activities. According to Dung et al. (2013), a PLI between 1 and 10 refers to a polluted environment. In this study, the unity of PLI (PLI = 1) was exceeded up to 2.5 times (in sample no. 31 – the base of the embankment), which reflects a deterioration of the soil quality. The values of CF and PLI for samples no. 27 (sand trap), no. 38, and no. 39 (drainage ditch) reflected only low to moderate deterioration of site quality, which indicates that a small amount of TMs were deposited in the

Table 4
The assessment of TM contamination status of soil samples using Contamination Factor (CF), Enrichment Factor (EF) and Pollution Load Index (PLI).

Sample	CF						EF						PLI
	Cr	Ni	Cu	Cd	Pb	Zn	Cr	Ni	Cu	Cd	Pb	Zn	
Test site 1													
11	3.7	1.3	5.5	0.2	3.9	1.3	4.5	1.6	6.7	0.3	4.8	1.6	1.8
12	5.6	1.1	1.8	0.2	1.4	0.8	6.4	1.2	2.1	0.2	1.6	0.9	1.2
13	4.8	1.5	4.8	0.6	3.7	3.8	3.8	1.2	3.8	0.4	2.9	1.7	2.3
Test site 2													
21	5.2	1.5	6.3	0.2	2.5	1.3	4.3	1.2	5.2	0.2	2.1	1.1	1.8
22	4.0	1.7	1.6	0.2	2.0	0.8	3.0	1.2	1.2	0.1	1.5	0.6	1.2
23	4.3	1.3	2.1	0.2	1.4	0.8	4.7	1.4	2.3	0.2	1.5	0.9	1.2
24	4.0	0.6	1.1	0.1	0.8	0.5	4.4	0.6	1.2	0.1	0.9	0.5	0.7
25	4.0	0.7	1.2	0.1	0.9	0.5	5.4	0.9	1.6	0.2	1.3	0.7	0.8
26	3.2	0.7	1.1	0.1	1.1	0.5	4.9	1.1	1.7	0.2	1.7	0.7	0.7
27	1.7	1.2	3.0	0.2	1.4	1.3	2.3	1.7	4.1	0.3	1.9	1.7	1.2
Test site 3													
31	3.9	0.9	34.5	0.3	3.9	1.3	4.0	1.0	36.1	0.4	4.1	1.4	2.5
32	3.9	1.5	6.2	0.5	4.0	2.0	5.1	1.9	8.2	0.7	5.3	2.6	2.3
33	3.4	1.1	2.7	0.2	2.3	0.8	4.5	1.5	3.6	0.2	3.1	1.0	1.2
34	4.0	1.5	2.9	0.2	1.6	1.2	2.0	0.8	1.4	0.1	0.8	0.6	1.3
35	4.2	2.3	8.2	0.3	4.9	1.7	3.4	1.9	6.7	0.2	4.0	1.4	2.4
36	2.8	0.9	3.2	0.2	2.9	2.5	4.1	1.3	4.6	0.3	4.2	3.7	1.6
37	4.2	1.5	5.1	0.4	3.5	1.6	4.5	1.6	5.4	0.4	3.7	1.7	2.0
38	2.1	1.4	2.5	0.1	1.0	0.8	3.5	2.3	4.3	0.2	1.7	1.3	1.0
39	3.1	1.3	2.6	0.1	1.3	0.5	7.1	3.1	5.9	0.1	2.9	1.1	0.9

Colors table cells represent the soil quality described in Tab.S1

sediment or that the redistribution of TMs involving surface runoff from embankments and railway construction is minor.

According to the EF classification (Table S.1), the anthropogenic contribution to the overall site contamination status was shown by the EF values for Cr, Cu, and Pb. For these TMs the EF values varied between 2.0–7.1, 1.2–36.1, and 0.8–5.3, respectively. The highest value was reported for Cu at Test site 3 (sample no. 31), indicating very severe enrichment. As shown in Table 4, the EF values of Ni, Cd, and Zn varied between 0.6–3.1, 0.1–0.7, and 0.5–3.7 respectively, with average values of 1.5, 0.3, and 1.3. In general the EF values for the analyzed TMs follow the descending order: Cu > Cr > Pb > Ni > Zn > Cd. Test site 1 was located close to a main road intersection of streets, and therefore the elevated Cu and Pb levels, when compared to Test site 2 (located 350 m away), could be explained by the impact of motor vehicles and traffic. In general, road deposited sediments (RDS) produced via vehicle wear-and-tear are a significant source of TMs. For example, Hong et al. (2018) reported the Cu and Pb content in RDS in the following ranges: 25.66–310.75 mg/kg and 15.61–220.35 mg/kg, respectively. In urban areas, the RDS could be set in motion by wind or air turbulence from traffic and transferred with dust to green areas, soil, as well as to plant leaves adjacent to the streets (Zafra et al., 2017).

Analysis of the CF and EF values clearly indicates enrichment of the analyzed soil samples with Cr, Cu, and Pb linked to anthropogenic activities, and thus potential pathways of these TMs into the environment deserve special attention. Cr is frequently a component of alloy steel used for rails, which may explain its abundance. However, other studies of railway-affected soils reported lower Cr enrichment in relation to background concentration (lower CF index) (Table 4).

3.4. Properties of railroad 248's construction and operation in regard to TM emissions

Particle emissions related to the wear of rails, vehicle wheels, brake blocks and discs, pantograph slide plates, and overhead contact lines (on electrified lines) or exhaust emissions (on non-electrified lines) are the main sources of TM pollution resulting from the operation and use of railway tracks. Due to the transfer of very high loads, rails wear along the vertical plane. Types of rail and steel alloys in current use significantly reduce the rate of vertical rail wear. In the curvilinear sections, there is additional friction of the wheel flange against the side surface of the railhead, which results in lateral wear. The greater the curvature of the track, the greater the wear. It is assumed that arcs with a radius of more than 3500 m can be treated as "slow wearing", and arcs with a radius of less than 1000 m as "fast wearing" (Santa et al., 2016). An additional parameter that affects the rate of lateral wear of the outer rail track is the cant deficiency, which depends on the curve radius, train speed, and the cant used (Pombo, 2012; Powell and Gräbe, 2017).

The commonly adopted practice to counteract intensified rail wear in curves is to use an appropriate rail steel alloy. According to the guidelines adopted by railway line No. 248 (PKM – 08), on arcs with a radius of 800 m or less, rails with strength $Rm \geq 1100$ MPa strength alloyed or heat-treated steel should be used. Such alloys are R350 HT (heat-treated according to PN-EN 13674-1 + A1:2017-07) or B1000 (alloyed). The alloy composition of rails with increased hardness has a higher content of metals such as Cr and Mn compared to typical rails made of R260 steel (according to the PN-EN 13674-1 + A1:2017-07 standard). In the investigated test sections, 49E1 rails made of heat-treated R350 HT steel (Test sections 1 and 2) and R260 steel (Test section 3) were used. The radius of the arch was 800 m (Test sections 1 and 2) and 3000 m (Test section 3). With an annual train traffic intensity of 1.5 Tg, it can be assumed that the rate of vertical rail wear is insignificant, while the side wear of the rails would be approximately 0.3 mm/year (Test section 1 and 2) and 0.05 mm/year (Test section 3).

Train wheels are made of ER7 steel (PN-EN 13260 + A1: 2011) or P54T steel (PN-ISO 1005-1: 2017-03). The vehicles running on the 248 railway line have monoblock wheelsets made of ER7 steel. The vertical

wear of the tread at this point is about 0.02 mm/1000 km, and the side wear of the flange is about 0.16 mm/1000 km (Muhamedsalih et al., 2019). The alloy composition of steels used in railways is shown in Table S.2.

In addition, parts of the braking system are subjected to heavy wear. The intensity of brake wear and the emission of particulate matter depends on the type of brake system: in the case of block brakes, the cast iron inserts and treads will wear out (Olofsson, 2011), while in the case of disc brakes, the composite brake blocks and discs are subjected to wear (Abbasi et al., 2011). Trains equipped with disc brakes, regenerative braking systems (with supercapacitors), and retarders, are currently running on the analyzed railway line. During normal service, trains use friction braking only in the final stopping phase only; therefore, along selected sections (on the route between stops), the impact of the wear of disc elements and pads on soil contamination may be ignored.

Hence, it can be concluded that the increased content of Cr and Cu may result from the wear of railway and vehicle wheels. This conclusion is consistent with research results collected by Abbasi et al. (2013) on the emission of solid particles in rail transport systems. The above-mentioned study showed that the PM2.5 and PM10 dust particles (not originating from the exhaust gas) have an average concentration of 0.142 μg/m^3 for Cr and 0.944 μg/m^3 for Cu. For Fe (which is the basic alloying component of steel), high concentrations were found - on average 30 μg/m^3. The last pollution source along railways, but not the least, is emission related to traction energy, which contributes Cu to the environment (Hai He et al., 1998). However, since electric power is not used, any source of Cu caused by the wearing of the current collector and contact wires can be excluded in the case of Railroad 248. Since the railway line in its current state has never been burdened with regular steam traction traffic (there have only been occasional trips made by historic steam locomotives), all pollution resulting from coal combustion comes from external emissions. The line is only now being prepared for electrification, so the source of pollution can solely be related to diesel engines.

3.5. Tracking analyses of TM sources

3.5.1. Correlation analyses between TMs

Spearman's correlation coefficients for analyzed TM concentrations are presented in Table 5. Significantly positive correlations were found between the following elemental pairs: Ni-Pb, Ni-Fe, Cu-Pb, Cd-Pb, Cd-Zn, and Pb-Zn. These results indicated that Ni, Cu, Cd, and Zn concentrations positively correlated with Pb concentrations, and thus those metals were likely to originate from common sources. Both elevated concentrations and high CF values of Cu and Pb in most soil samples indicate potential anthropogenic origin. In addition, Chen et al. (2014) noted a similar anthropogenic source for the Cd-Pb pair. There was no correlation between Cr and any other TM concentrations. At the same time, both CFs and EFs calculated for Cr pointed to considerable and moderate contamination status, respectively. This could suggest supplementation of Cr from a different source than other metals, and railroad 248 seems to be the most likely.

CA results presented in Fig. 2 divide the analyzed TMs into two groups with the significant association: a) group "a" consisting of Zn, Pb, and Cd within a close distance (<0.3 of height) and b) group "b" containing Fe and Ni within approx. 0.4 height. Cu demonstrated a relationship with group "a", while Cr did so with group "b". A more significant correlation was related to a lower cluster distance (Zhang et al., 2012). Moreover, elements within the same group are expected to exhibit a common anthropogenic or natural source (Khan et al., 2011). Zn, Pb, and Cd are widely regarded as indicator metals in contaminated soils near highways (Wang et al., 2011). However, Zhang et al. (2012) noted that Zn, Pb, and Cd could also be delivered to the soil from rail traffic. TMs belonging to group "a" are undoubtedly correlated with anthropogenic activity. Group "b" could be associated with the natural

Table 5
Spearman's correlation matrix between the seven TMs for soil samples collected from railroad 248 embankments.

Element	Cr	Ni	Cu	Cd	Pb	Zn	Fe
Cr	1.00						
Ni	0.23	1.00					
Cu	0.03	0.01	1.00				
Cd	0.17	0.37	0.33	1.00			
Pb	0.12	**0.60**	**0.51**	**0.70**	1.00		
Zn	-0.07	0.42	0.23	**0.73**	**0.74**	1.00	
Fe	0.36	**0.56**	0.03	0.05	0.08	0.09	1.00

Bold – significant correlation

occurrence of these metals in the environment because of the low content of Ni and Fe in several analyzed samples. However, the distances within group "b" were higher than those within group "a", which calls into question a common origin of metals from group "b". This is supported by the results of correlation analysis, which demonstrated Cr to be an outlier from the whole group of TMs. The statistical analyses, despite their importance, are useful for initial TM classification, although they require further verification. Here, Pb isotopic analysis was performed.

3.5.2. Pb isotope ratios

The application of Pb isotope ratios to track contamination is one of the most promising new areas of environmental geochemistry (Mihaljevic et al., 2019). The Pb isotope ratios of $^{206}Pb/^{207}Pb$ and $^{208}Pb/^{206}Pb$ for the analyzed soil samples, with reference to Pb isotope ratios observed for different anthropogenic sources, are presented in Fig. 3a. The obtained results are 1.16–1.20 for $^{206}Pb/^{207}Pb$ and 2.05–2.10 for $^{208}Pb/^{206}Pb$. In general these ranges correspond to anthropogenic supplementation of Pb. The soil samples collected at Test site 1, and most samples collected from Test site 3, are indicated to have coal combustion and leaded gasoline sources of origin. Test site 2, which is located further away, is also affected by coal combustion. In Poland, the heating systems are mainly coal-fired and therefore associated with high emissions. Despite the implementation of a number of environment-oriented programs to reduce the burden of emissions

(e.g. change to a gas furnace or minimum class 5 heat boilers according to PN-EN 303-5:2012), the problem is still relevant in most municipalities. Polish cities are regularly classified in the top 10 European cities with the worst air quality, and this ignominious position is largely due to low-rise buildings high emission (EEA Report, 2020). Airborne pollutants can be transferred to different sites of cities, and outside cities, and deposited there. Regarding gasoline, unleaded petrol is normally used in Poland. However, according to national standards and regulations, unleaded gasoline still contains a Pb additive, though the maximum concentration is limited to 5 mg/L. Diesel fuel does not contain Pb additives, and therefore Pb supplementation from locomotive fuel can be excluded. However, the possibility of leakage or wearing of mechanical
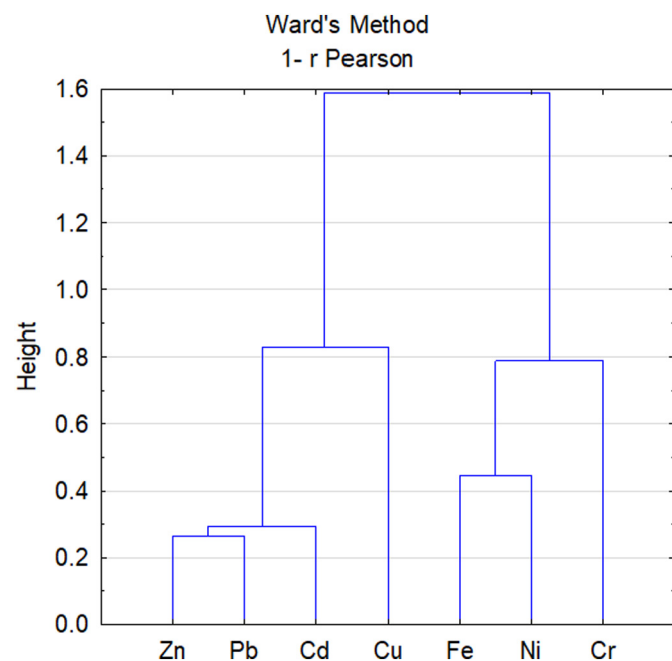

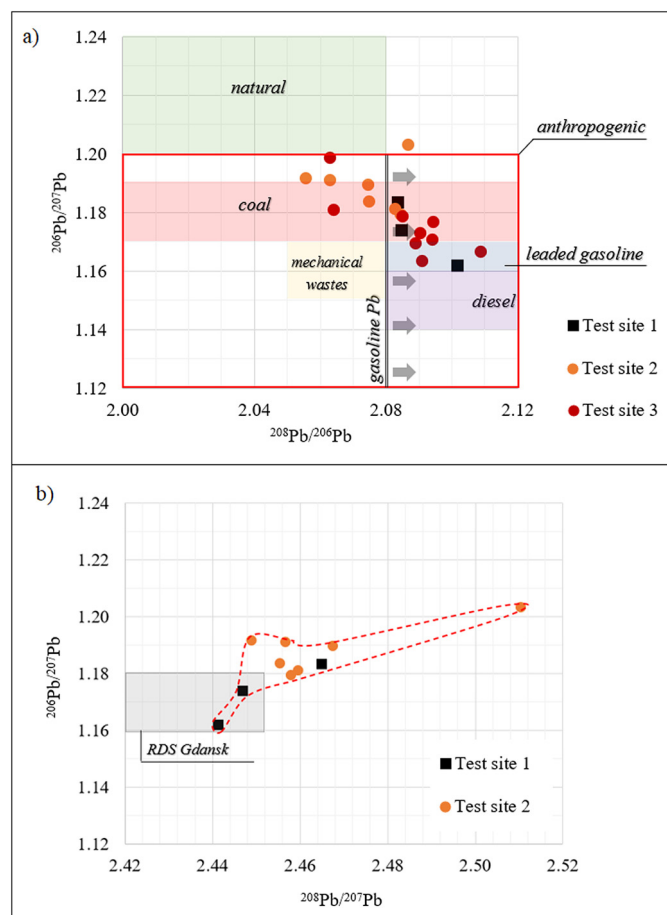**Fig. 3.** A schematic of a three-isotope plot: a) ($^{206}Pb/^{207}Pb$ vs. $^{208}Pb/^{206}Pb$) showing the isotopic composition of different Pb sources vs. the results noted for soil samples near the railway - grey arrows indicate $^{208}Pb/^{206}Pb$ ratio for the contribution of gasoline Pb; and b) ($^{206}Pb/^{207}Pb$ vs. $^{208}Pb/^{207}Pb$) showing the Pb isotope ratio for road deposited sediments (RDS) collected in Gdansk (Nawrot et al., 2020a) close to Test sites 1 and 2 vs. the results obtained for soil samples near the railway.

Fig. 2. Cluster dendrogram of elements showing interrelationships among metals.

parts in the train composition should also be considered as a potential pathway of Pb supplementation.

Fig. 3b presents the $^{206}Pb/^{207}Pb$ vs. $^{208}Pb/^{207}Pb$ isotopic ratios for railway soil samples together with the ranges of Pb isotopic ratios reported by Nawrot et al. (2020a) for RDS collected from the intersection located in the vicinity of Test sites 1 and 2. The results obtained for soil samples from Test site 1 mostly cover the ranges of Pb isotopic ratios obtained for *RDS Gdansk* (Fig. 3b), which means that this site is also supplemented with Pb and Pb correlated TMs (Zn, Ni, Cr) by road transport. The mixed sources of TM supplementation at this site are justified by the close proximity of an intersection of main roads with associated heavy traffic. Moreover, the Pb isotopic ratios $^{206}Pb/^{207}Pb$ and $^{208}Pb/^{207}Pb$ reported by Nawrot et al. (2020b) for bottom sediments in a nearby surface runoff receiver (retention tank Potokowa in Gdansk, 50 m from Test site 1: 1.16–1.19 for $^{206}Pb/^{207}Pb$ and 2.42–2.46 $^{208}Pb/^{207}Pb$) were at similar levels to those observed for Test site 1 and 2. Hence, railroad 248 could be an additional source of Pb and Pb correlated TM supplementation.

To sum up, the source tracking methods performed within this study lead to the following observations:

- Mixed sources including coal combustion, road transport, and railroad 248 contribute to the supplementation of Zn, Pb, Cd, and, partly, Cu;
- Natural occurrence with some minor interference from coal combustion is likely in the case of Ni and Fe;
- Railroad 248 is a distinctive source of Cr supplementation.

3.6. Prospective soil remediation options

Soils contaminated with TMs should be remediated to mitigate the toxic impact on the environment. In general, the remediation options can be divided into in-situ and ex-situ technologies. In-situ remediation can be performed at the contaminated site without excavation and transport of the contaminated soil to off-site treatment facilities. These methods include surface capping, soil flushing, encapsulation, electrokinetic extraction, chemical immobilization, as well as more ecological approaches such as phytoremediation and bioremediation (Liu et al., 2018a). Among the in-situ methods, chemical immobilization of pollutants in the contaminated soil by application of chemical agents or phyto- and bioremediation methods may be the most advantageous for use along railway tracks (Zalesny et al., 2021). The vegetation cover of railway cut slopes and plant protection strips can contribute to reduction of soil contamination along the railway line as well as reduction of its spread (Hoerbinger et al., 2020). Ex-situ methods (such as landfilling, or "dig and haul", soil washing, solidification, or vitrification) rely on the excavation of soil from the contaminated site, transport of the contaminated soil to an off-site treatment facility, and disposal of the treated soil. Therefore, such methods require extra costs for soil excavation, transport, disposal, and site refilling (Koul and Taak, 2018).

To sum up, proper track maintenance and the use of green methods to mitigate the spread of contaminants related to rail operations are crucial for reducing soil contamination. The process of redistribution of the dust generated during wear of the rails and wheels involves particles settling on the ballast bed and on the surfaces of embankments and ditches. It is also important to protect the final receiver from contaminants forming while run-off seeps through the track. During dry periods, the contaminants deposit on the ballast, and then during wet periods they filter through the blanket, consisting of a sand and gravel mix of 0–31.5 mm aggregate, on which larger particles are deposited. The water then flows down on the surface of the embankment to its base. The embankment surfaces are covered with low-growing vegetation which, apart from advantageous properties related to the absorption of dust, reduces the speed of water runoff along sharply inclined embankments, and in turn reduces the rate of washing away of soil grains. The water is then collected into longitudinal drainage ditches, the bottom of which has a suitable slope enabling further water flow

along the ditch. At the lowest points of the grade line of the ditch, there are water outlets to watercourses or rainwater drainage. In the case of the analyzed railway line No. 248, these are equipped with various types of technical devices (such as sand traps, settling tanks, or oil-derivative substance separators) to protect the rainwater drainage system against silting and to prevent environmental pollution.

4. Conclusions

TM concentrations at three test sites in the immediate vicinity of railroad 248 in Gdansk were examined. Collected samples had an elevated TM content and can be classified as being 'highly' contaminated (with respect to Cu) or 'moderately severely' contaminated (with respect to Pb, Cr, and Zn), or having 'moderate to low' contamination levels (with respect to Ni and Cd). In comparison to the results of other studies, in this research exceptionally high levels of Pb (max. 80.5 mg/kg d.w.) were noted, while Ni and Cd concentrations were rather low (max. 13.2 and 0.282 mg/kg d.w., respectively). The extensive source tracking analyses covered statistical analyses and Pb isotope ratios which, when used simultaneously, made it possible to accurately verify the sources of metals. Correlation analyses allowed TMs to be divided into two general groups: a) containing Zn, Pb, Cd with slight interaction with Cu; and b) containing Fe and Ni with slight interaction with Cr. These analyses also pointed to Cr as a standout TM delivered from a separate source, which may be associated with the specificity of the construction of railroad 248 and the use of Cr-containing alloys to counteract heavy rail wear. Pb isotopic ratios in the ranges of 1.16–1.20 $^{206}Pb/^{207}Pb$ and 2.05–2.10 $^{208}Pb/^{206}Pb$ corresponded to anthropogenic supplementation of Pb and Pb-correlated TMs. In general, Pb was supplemented from coal combustion, unleaded gasoline (which still contains a Pb additive), as well as by leakage or wear of mechanical parts from the train's composition. As Zn, Pb, Cd, and partly Cu were correlated to Pb, they probably have the same mixed origin sources. Despite the research focus on the impact of the railroad contribution, road transport appeared to have a higher contributing factor to TM pollution at the investigated sites. This general conclusion again emphasizes the smaller environmental footprint left by railway transport in comparison to road transport.

Appendix A. Supplementary data

Supplementary data to this article can be found online at https://doi.org/10.1016/j.scitotenv.2021.149300.

References

Abbasi, S., Jansson, A., Sellgren, U., Olofsson, U., 2013. Particle emissions from rail traffic: a literature review. Crit. Rev. Environ. Sci. Technol. 43 (23), 2511–2544. https://doi.org/10.1080/10643389.2012.685348.

Abbasi, S., Wahlström, J., Olander, L., Larsson, C., Olofsson, U., Sellgren, U., 2011. A study of airborne wear particles generated from organic railway brake pads and brake discs. Wear 273 (1), 93–99.

Adamiec, E., Jarosz-Krzeminska, E., Wieszala, R., 2016. Heavy metals from non-exhaust vehicle emissions in urban and motorway road dusts. Environ. Monit. Assess. 188. https://doi.org/10.1007/s10661-016-5377-1.

Brtnický, M., Pecina, V., Baltazár, T., Galiová, M.V., Baláková, L., Bes, A., Radziemska, M., 2020. Environmental impact assessment of potentially toxic elements in soils near the runway at the international airport in Central Europe. Sustainability 12 (17), 1–14. https://doi.org/10.3390/su12172224.

Budzynski, M., Szmaglinski, J., Jamroz, K., Birr, K., Grulkowski, S., Wachnicka, J., 2019. Assessing tram infrastructure safety using the example of the City of Gdansk. J. KONBiN 49, 293–322. https://doi.org/10.2478/jok-2019-0060.

Cheema, A.I., Liu, G., Yousaf, B., Abbas, Q., Zhou, H., 2020. A comprehensive review of biogeochemical distribution and fractionation of lead isotopes for source tracing in distinct interactive environmental compartments. Sci. Total Environ. 719, 135658. https://doi.org/10.1016/j.scitotenv.2019.135658.

Chen, X., Xia, X., Zhao, Y., Zhang, P., 2010. Heavy metal concentrations in roadside soils and correlation with urban traffic in Beijing, China. J. Hazard. Mater. 181, 640–646. https://doi.org/10.1016/j.jhazmat.2010.05.060.

Chen, Z., Wang, K., Wei Ai, Y., Li, W., Gao, H., Fang, C., 2014. The effects of railway transportation on the enrichment of heavy metals in the artificial soil on railway cut slopes. Environ. Monit. Assess. 186, 1039–1049. https://doi.org/10.1007/s10661-013-3437-3.

Chrastný, V., Šillerová, H., Vítková, M., Francová, A., Jehlicka, J., Kocourková, J., Aspholm, P.E., Nilsson, L.O., Berglen, T.F., Jensen, H.K.B., Komárek, M., 2018. Unleaded gasoline as a significant source of Pb emissions in the subarctic. Chemosphere 193, 230–236. https://doi.org/10.1016/j.chemosphere.2017.11.031.

Crosby, C.J., Fullen, M.A., Booth, C.A., Searle, D.E., 2014. A dynamic approach to urban road deposited sediment pollution monitoring (marylebone road, London, UK). J. Appl. Geophys. 105, 10–20. https://doi.org/10.1016/j.jappgeo.2014.03.006.

Dung, T.T.T., Cappuyns, V., Swennen, R., Phung, N.K., 2013. From geochemical background determination to pollution assessment of heavy metals in sediments and soils. Rev. Environ. Sci. Biotechnol. 12, 335–353. https://doi.org/10.1007/s11157-013-9315-1.

EC EUROPA, d. https://ec.europa.eu/eurostat/statisticsexplained/index.php/Freight_transport_statistics_-_modal_split (accessed on 15 January 2021).

EEA EUROPA, d. https://www.eea.europa.eu/data-and-maps/data/external/modal-split-of-passenger-transport-eurostat (accessed on 15 January 2021).

EEA Report, 2020. Air Quality in Europe — 2020 Report accessed on 21 January 2021.

Gao, L., Han, L., Peng, W., Gao, B., Xu, D., Wan, X., 2018. Ecotoxicology and environmental safety identification of anthropogenic inputs of trace metals in lake sediments using geochemical baseline and Pb isotopic composition. Ecotoxicol. Environ. Saf. 164, 226–233. https://doi.org/10.1016/j.ecoenv.2018.08.014.

GeoLOG application, d. https://geolog.pgi.gov.pl/ (Accessed on 3rd November 2020).

German, J., Svensson, G., 2018. Metal Content and Particle Size Distribution of Street Sediments and Street Sweeping Waste 191–198.

González-Macías, C., Sánchez-Reyna, G., Salazar-Coria, L., Schifter, I., 2014. Application of the positive matrix factorization approach to identify heavy metal sources in sediments. A Case Study on the Mexican Pacific Coast. 307–324. https://doi.org/10.1007/s10661-013-3375-0.

Goth, A., Michelsen, A., Rousk, K., 2019. Railroad derived nitrogen and heavy metal pollution does not affect nitrogen fixation associated with mosses and lichens at a tundra site in Northern Sweden. Environ. Pollut. 247, 857–865. https://doi.org/10.1016/j.envpol.2019.01.101.

Hai He, D., Manory, R.R., Grady, N., 1998. Wear of railway contact wires against current collector materials. Wear 215 (1–2), 146–155. https://doi.org/10.1016/S0043-1648(97)00262-7.].

Hakanson, L., 1980. An ecological risk index for aquatic pollution control. A sedimentological approach. Water Res. 14, 975–1001. https://doi.org/10.1016/0043-1354(80)90143-8.

Hoerbinger, S., Obriejetan, M., Rauch, H.P., Immitzer, M., 2020. Assessment of safety-relevant woody vegetation structures along railway corridors. Ecol. Eng. 158, 106048. https://doi.org/10.1016/j.ecoleng.2020.106048.

Hong, N., Zhu, P., Liu, A., Zhao, X., Guan, Y., 2018. Using an innovative flag element ratio approach to tracking potential sources of heavy metals on urban road surfaces. Environ. Pollut. 243, 410–417. https://doi.org/10.1016/j.envpol.2018.08.098.

Jamroz, K., Budzynski, M., Romanowska, A., Zukowska, J., Oskarbski, J., Kustra, W., 2019. Experiences and challenges in fatality reduction on polish roads. Sustainability 11, 959. https://doi.org/10.3390/su11040959.

Johansson, C., Norman, M., Burman, L., 2008. Road traffic emission factors for heavy metals. Atmosph. Environ. 43, 4681–4688. https://doi.org/10.1016/j.atmosenv.2008.10.024.

Khan, M.N., Wasim, A.A., Sarwar, A., Rasheed, M.F., 2011. Assessment of heavy metal toxicants in the roadside soil along the N-5, National Highway, Pakistan. Environ. Monit. Assess. 182, 587–595.

Komárek, M., Chrastný, V., Mihaljevi, M., 2008. Lead Isotopes in Environmental Sciences: A Review 34, 562–577. https://doi.org/10.1016/j.envint.2007.10.005.

Kowalska, J.B., Mazurek, R., Gasiorek, M., Zaleski, T., 2018. Pollution indices as useful tools for the comprehensive evaluation of the degree of soil contamination–a review. Environ. Geochem. Health 1–26. https://doi.org/10.1007/s10653-018-0106-z.

Koul, B., Taak, P., 2018. Ex situ soil remediation strategies. Biotechnological Strategies for Effective Remediation of Polluted Soils https://doi.org/10.1007/978-981-13-2420-8_3.

Kustra, W., Zukowska, J., Budzynski, M., Jamroz, K., 2019. Injury prediction model for onshore road network development. Pol. Marit. Res. 2 26, 93–103. https://doi.org/10.2478/pomr-2019-0029.

Lisiak-Zielinska, M., Borowiak, K., Budka, A., Kanclerz, J., Janicka, E., Kaczor, A., Zyromski, A., Biniak-Pieróg, M., Podawca, K., Mleczek, M., Niedzielski, P., 2021. How polluted are cities in Central Europe? - Heavy metal contamination in Taraxacum officinale and soils collected from different land use areas of three representative cities. Chemosphere 266, 129113. https://doi.org/10.1016/j.chemosphere.2020.129113.

Liu, L., Li, W., Song, W., Guo, M., 2018a. Remediation techniques for heavy metal-contaminated soils: principles and applicability. Sci. Total Environ. 633, 206–219. https://doi.org/10.1016/j.scitotenv.2018.03.161.

Liu, A., Ma, Y., Gunawardena, J.M.A., Egodawatta, P., Ayoko, G.A., Goonetilleke, A., 2018b. Heavy metals transport pathways: the importance of atmospheric pollution contributing to stormwater pollution. Ecotoxicol. Environ. Saf. 164, 696–703. https://doi.org/10.1016/j.ecoenv.2018.08.072.

Liu, S., Zhan, C., Zhang, J., Liu, H., Xiao, Y., Zhang, L., Guo, J., Liu, G., Xing, X., Cao, J., 2020. Polycyclic aromatic hydrocarbons in railway stations dust of the mega traffic hub city, Central China: human health risk and relationship with black carbon. Ecotoxicol. Environ. Saf. 205.

Loxham, M., Nieuwenhuijsen, M.J., 2019. Health effects of particulate matter air pollution in underground railway systems- a critical review of the evidence. Part. Fibre Toxicol. 16, 1–24. https://doi.org/10.1186/s12989-019-0296-2.

Mihaljevic, M., Baieta, R., Ettler, V., Vanek, A., Kríbek, B., Penížek, V., Drahota, P., Trubac, J., Sracek, O., Chrastný, V., Siyowi, B., 2019. Tracing the metal dynamics in semi-arid soils near mine tailings using stable Cu and Pb isotopes. Chem. Geol. 515, 61–76. https://doi.org/10.1016/j.chemgeo.2019.03.026.

Minister of the Environment, 2016. Regulation of the minister of the environment on the assessment method of the earth's surface pollution, 2016. Poland. J. Laws Repub. Pol. 1–86.

Mohsen, M., Ahmed, M.B., Zhou, J.L., 2018. Particulate matter concentrations and heavy metal contamination levels in the railway transport system of Sydney, Australia. Transp. Res. Part D Transp. Environ. 62, 112–124. https://doi.org/10.1016/j.trd.2018.02.015.

Muhamedsalih, Y., Stow, J., Bevan, A., 2019. Use of railway wheel wear and damage prediction tools to improve maintenance efficiency through the use of economic tire turning. Proc. Inst. Mech. Eng. F J. Rail Rapid Transit 233 (1), 103–117. https://doi.org/10.1177/0954409718781127.

Nawrot, N., Wojciechowska, E., Rezania, S., Walkusz-Miotk, J., Pazdro, K., 2020a. The effects of urban vehicle traffic on heavy metal contamination in road sweeping waste and bottom sediments of retention tanks. Sci. Total Environ. 749, 141511. https://doi.org/10.1016/j.scitotenv.2020.141511.

Nawrot, N., Wojciechowska, E., Matej-Lukowicz, K., Walkusz-Miotk, J., Pazdro, K., 2020b. Spatial and vertical distribution analysis of heavy metals in urban retention tanks sediments: a case study of Strzyza Stream. Environ. Geochem. Health 8. https://doi.org/10.1007/s10653-019-00439-8.

Nieuwenhuijsen, M.J., Gómez-Perales, J.E., Colvile, R.N., 2007. Levels of particulate air pollution, its elemental composition, determinants and health effects in metro systems. Atmos. Environ. 41, 7995–8006. https://doi.org/10.1016/j.atmosenv.2007.08.002.

Olofsson, U., 2011. A study of airborne wear particles generated from the train traffic—block braking simulation in a pin-on-disc machine. Wear 271 (1–2), 86–91. https://doi.org/10.1016/j.wear.2010.10.016.

Regulation of the Minister of Transport and Maritime Economy, 1998. Concerning on the technical conditions which railroad structures and their location should correspond to, Warsaw. (in Polish). http://isap.sejm.gov.pl/isap.nsf/DocDetails.xsp?id=WDU19981510987.

Pal, S.K., Wallis, S.G., Arthur, S., 2010. Assessment of heavy metals emission from traffic on road surfaces. Cent. Eur. J. Chem. 9, 314–319. https://doi.org/10.2478/s11532-011-0005-y.

PKM-08, 2014. Instruction of Technical Conditions for Construction and Maintenance of the Railway Tracks, Gdansk (in Polish).

Padoan, E., Romè, C., Ajmone-Marsan, F., 2017. Bioaccessibility and size distribution of metals in road dust and roadside soils along a peri-urban transect. Sci. Total Environ. 601–602, 89–98. https://doi.org/10.1016/j.scitotenv.2017.05.180.

Pombo, J., 2012. Application of a computational tool to study the influence of worn wheels on railway vehicle dynamics. J. Softw. Eng. Appl. 5 (2), 51–61. https://doi.org/10.4236/jsea.2012.52009.

Powell, A.F., Gräbe, P.J., 2017. Exploring the relationship between vertical and lateral forces, speed and superelevation in railway curves. J. South Afr. Inst. Civil Eng. 59 (3), 25–35. https://doi.org/10.17159/2309-8775/2017/v59n3a4.

Radziemska, M., Gusiatin, Z.M., Kowal, P., Bes, A., Majewski, G., Jeznach-Steinhagen, A., Mazur, Z., Liniauskiene, E., Brtnický, M., 2020. Environmental impact assessment of risk elements from railway transport with the use of pollution indices, a biotest and bioindicators. Hum. Ecol. Risk. Assess., 1–24 https://doi.org/10.1080/10807039.2020.1736984.

Ray, S., Khillare, P.S., Kim, K.H., 2012. The effect of aircraft traffic emissions on the soil surface contamination analysis around the international airport in Delhi, India. Asian J. Atmos. Environ. 6, 118–126. https://doi.org/10.5572/ajae.2012.6.2.118.

Sakan, S., Devic, G., Relic, D., Andelkovic, I., Sakan, N., Đordevic, D., 2014. Evaluation of sediment contamination with heavy metals: the importance of determining appropriate background content and suitable element for normalization. Environ. Geochem. Health 37, 97–113. https://doi.org/10.1007/s10653-014-9633-4.

Santa, J.F., Toro, A., Lewis, R., 2016. Correlations between rail wear rates and operating conditions in a commercial railroad. Tribo. Int. 95, 5–12. https://doi.org/10.1016/j.triboint.2015.11.003.

StatSoft Statistica 13, d. https://www.statsoft.pl/statistica_13/.

Stojic, N., Pucarevic, M., Stojic, G., 2017. Railway transportation as a source of soil pollution. Transp. Res. Part D Transp. Environ. 57, 124–129. https://doi.org/10.1016/j.trd.2017.09.024.

Sun, J., Yu, R., Hu, G., Su, G., Zhang, Y., 2018. Catena Tracing of heavy metal sources and mobility in a soil depth pro fi le via isotopic variation of Pb and Sr. Catena 171, 440–449. https://doi.org/10.1016/j.catena.2018.07.040.

Tomlinson, D.L., Wilson, J.G., Harris, C.R., Jeffrey, D.W., 1980. Problems in the assessment of heavy-metal levels in estuaries and the formation of a pollution index. Helgoländer Meeresuntersuchungen 33, 566–575. https://doi.org/10.1007/BF02414780.

Vallius, H., Leivuori, M., 1999. The distribution of heavy metals and arsenic in recent sediments in the Gulf of Finland. Boreal Environ. Res. 4, 19–29.

Via Vistula, 2016. Gdansk Traffic Study. (in Polish). https://www.brg.gda.pl/planowanie-przestrzenne/inne-opracowania-urbanistyczne/282-gdanskie-badania-ruchu-2016.

Wang, M.E., Markert, B., Chen, W.P., Peng, C., Ouyang, Z.Y., 2011. Identification of heavy metal pollutants using multivariate analysis and effects of land uses on their accumulation in urban soils in Beijing, China. Environ. Monit. Assess. https://doi.org/10.1007/s10661- 011-2388-9.

Wang, Y., Yang, L., Kong, L., Liu, E., Wang, L., Zhu, J., 2015. Spatial distribution, ecological risk assessment and source identification for heavy metals in surface sediments from Dongping Lake, Shandong, East China. Catena 125, 200–205. https://doi.org/10.1016/j.catena.2014.10.023.

Weerakkody, U., Dover, J.W., Mitchell, P., Reiling, K., 2017. Particulate matter pollution capture by leaves of seventeen living wall species with special reference to rail-traffic at a metropolitan station. Urban For. Urban Green. 27, 173–186. https://doi.org/10.1016/j.ufug.2017.07.005.

Weissmannová, H.D., Pavlovský, J., 2017. Indices of soil contamination by heavy metals – methodology of calculation for pollution assessment (minireview). Environ. Monit. Assess. 189. https://doi.org/10.1007/s10661-017-6340-5.

Werkenthin, M., Kluge, B., Wessolek, G., 2014. Metals in European roadside soils and soil solution - a review. Environ. Pollut. 189, 98–110. https://doi.org/10.1016/j.envpol.2014.02.025.

Wojciechowska, E., Nawrot, N., Matej-Lukowicz, K., Gajewska, M., Obarska-Pempkowiak, H., 2019a. Seasonal changes of the concentrations of mineral forms of nitrogen and phosphorus in watercourses in the agricultural catchment area (Bay of Puck, Baltic Sea, Poland). Water Sci. Technol. Water Supply 19. https://doi.org/10.2166/ws.2018.190.

Wojciechowska, E., Nawrot, N., Walkusz-Miotk, J., Matej-Lukowicz, K., Pazdro, K., 2019b. Heavy metals in sediments of urban streams: contamination and health risk assessment of influencing factors. Sustainability 11, 563. https://doi.org/10.3390/su11030563.

Yan, G., Mao, L., Liu, S., Mao, Y., Ye, H., Huang, T., Li, F., Chen, L., 2018. Enrichment and sources of trace metals in roadside soils in Shanghai, China: a case study of two urban/rural roads. Sci. Total Environ. 631–632, 942–950. https://doi.org/10.1016/j.scitotenv.2018.02.340.

Yao, P.H., Shyu, G.S., Chang, Y.F., Chou, Y.C., Shen, C.C., Chou, C.S., Chang, T.K., 2015. Lead isotope characterization of petroleum fuels in Taipei, Taiwan. Int. J. Environ. Res. Public Health 12, 4602–4616. https://doi.org/10.3390/ijerph120504602.

Zaborska, A., 2014. Anthropogenic lead concentrations and sources in Baltic Sea sediments based on lead isotopic composition. Mar. Pollut. Bull. 85, 99–113. https://doi.org/10.1016/j.marpolbul.2014.06.013.

Zaborska, A., Zawierucha, K., 2016. Chemosphere Accumulation of Atmospheric Radionuclides and Heavy Metals in Cryoconite Holes on an Arctic Glacier. 160, pp. 162–172. https://doi.org/10.1016/j.chemosphere.2016.06.051.

Zafra, C., Temprano, J., Tejero, I., 2017. The physical factors affecting heavy metals accumulated in the sediment deposited on road surfaces in dry weather: a review. Urban Water J. 9006, 1–11. https://doi.org/10.1080/1573062X.2016.1223320.

Zalesny, R.S., Casler, M.D., Hallett, R.A., Lin, C.-H., Pilipovic, A., 2021. Bioremediation and soils Chapter 9. Soils and Landscape Restoration https://doi.org/10.1016/b978-0-12-813193-0.00009-6.

Zhang, H., Wang, Z., Zhang, Y., Hu, Z., 2012. The effects of the Qinghai – Tibet railway on heavy metals enrichment in soils. Sci. Total Environ. 439, 240–248. https://doi.org/10.1016/j.scitotenv.2012.09.027.